Structural components of the Pt/Si(111)-($\sqrt{3}\times\sqrt{3}$) surface from scanning tunneling microscopy

P. Höpfner, M. Wisniewski, F. Sandrock, J. Schäfer, and R. Claessen
Physikalisches Institut, Universität Würzburg, 97074 Würzburg, Germany

(Received 23 December 2009; revised manuscript received 16 June 2010; published 31 August 2010)

From topographic inspection of the ($\sqrt{3}\times\sqrt{3}$)-Pt/Si(111) surface by scanning tunneling microscopy, key structural elements are identified. A characteristic triangular building block in each ($\sqrt{3}\times\sqrt{3}$) unit cell, composed of charge maxima at approximately the bulk Pt-Pt distance bond, is observed. The orientation of the trimers is incompatible with the Si(111) substrate symmetry, which becomes obvious at domain-wall boundaries. In consequence, a simple top-layer trimer model is rendered insufficient. Instead, the finding of rotated trimers points at a more complex rearrangement of the surface, which generates the observed symmetry-breaking structural relaxation that leads to a chiral surface.

DOI: 10.1103/PhysRevB.82.075431 PACS number(s): 68.35.−p, 68.37.Ef, 68.55.−a, 61.46.−w

I. INTRODUCTION

Two-dimensional electron systems (2DESs) may be used as model systems for the study of physical phenomena in reduced dimensions. Such systems can, e.g., be realized by a coating of one monolayer (ML) or less of metal adsorbate atoms on a (111)-oriented semiconductor surface.[1–3] In principle, the localization of charge carriers is adjusted by the choice of substrate and adsorbate composition. As a consequence of the limited dimensions, electron correlation effects are no longer negligible, which might therefore trigger a Mott-Hubbard metal-insulator transition.[4] Moreover, a charge-density wave may occur for suitable Fermi-surface topologies in the presence of electron-phonon coupling, and might be expected to be observed in such surface systems.[5]

Metal adatoms on a (111) semiconductor often render the surface ($\sqrt{3}\times\sqrt{3}$)-reconstructed (abbreviated $\sqrt{3}$). Therefore, these surface reconstructions have been studied for several atom species.[6–8] Such systems often possess narrow surface bands so that on-site Coulomb repulsion plays a significant role. Thus, they mark an ideal playground to study correlation effects in two dimensions. Especially, the $\sqrt{3}$ structure of the group IV adatoms Sn and Pb on Si(111) and Ge(111) has attracted a lot of attention since the discovery of the ($\sqrt{3}\times\sqrt{3}$)$\rightarrow$(3×3) phase transition of the dilute Pb/Ge(111) α-phase in 1996.[1] Calculations within the local spin-density approximation, including the Hubbard U were performed on the closely related Sn/Si(111) and Sn/Ge(111) systems. These arrived at a Mott insulating ground state,[9] which is also observed in experiment.[10,11] Moreover, there is speculation that, based on strong electron correlations, superconductivity might occur in such systems at low temperature.[9]

Besides the group IV adsorbates, noble-metal adatoms are suitable to generate a $\sqrt{3}$ reconstructed 2DES. These contribute d and s orbitals to the overall electronic configuration, which extends the variety of 2DESs with different properties. A key question in the noble-metal-based $\sqrt{3}$ reconstruction is the local atomic structure, which lies at the very heart of the potentially exotic electronic properties. Three alternative structural models have been promoted, thus far with evidence based on Ag- and Au-induced structures. The different $\sqrt{3}$ reconstructions of Ag/Si(111) and Au/Si(111) are generally assumed to be formed at a nominal coverage of 1 ML.[8]

An intriguing, yet only sparsely examined example of noble-metal-induced surface reconstructions is $\sqrt{3}$-Pt/Si(111), which is in the focus of the present paper. Unlike silver and gold, platinum features an open d shell. Most experimental studies of the Pt/Si(111) interface concern the high coverage regime up to 40 ML.[12,13] At low coverage, $\sqrt{3}$-Pt/Si(111) has been characterized by electron-diffraction experiments in 1980s.[14–16] Recent studies provide scanning tunneling microscopy (STM) data with atomic resolution between platinum silicide islands.[17,18] But up to today the coverage of this reconstruction is not known definitely, although Morgen *et al.* claim the coverage to be 1/3 ML.[16] Apart from these structural aspects, the electronic structure remains unidentified due to a lack of, e.g., angle-resolved photoelectron spectroscopy (ARPES) experiments.

In this paper, we present a STM study of $\sqrt{3}$-Pt/Si(111) in the low Pt coverage regime as an approach to the atomic properties of this surface. A large area reconstruction with three different orientations, divided by phase-slip domain walls, is observed. Our STM data show resemblance to $\sqrt{3}$-Au/Si(111) and give indication of a conjugated honeycomb chained trimer (CHCT) configuration. Most notably, the evaluation of the atomic arrangement in the vicinity of domain walls strongly suggests that the Pt trimers are rotated with respect to the substrate, hence giving rise to a chirality of the surface. Furthermore, this work points at a 1 ML coverage within the $\sqrt{3}$-reconstructed domains.

This paper is organized in the following sections: after the experimental procedures in Sec. II, we present in Sec. III an overview of the STM image situation, which indicates the ubiquitous presence of domain boundaries in $\sqrt{3}$-Pt/Si(111). In Sec. IV, we address in detail the major structural units both in the domain as well as at the domain wall. From these data key ingredients for a structural model are derived. The main conclusions are summarized in Sec. V.

II. EXPERIMENTAL

Experiments were carried out in an ultrahigh vacuum system with a base pressure lower than 1×10^{-10} mbar. The surface analysis chamber is equipped with a variable-temperature scanning tunneling microscope (Omicron Nano-Technology).

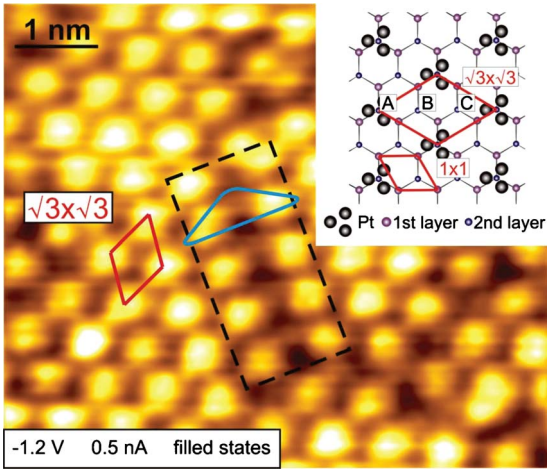

FIG. 1. (Color online) STM image of $\sqrt{3}$-Pt/Si(111) for filled states (−1.2 V) at 300 K (6.5×5.6 nm^2). Reconstructed domains (mean size ~10 nm^2) are divided by phase-slip domain boundaries, which appear darker. The rhomboid represents the $\sqrt{3}$ unit cell, the dashed rectangle marks a domain boundary, and the triangle highlights the domain-wall building unit (see discussion in Sec. IV B). The inset illustrates the geometric origin of the phase-slip domain boundaries: With regard to the (1×1) substrate unit cell, the $\sqrt{3}$ unit cell can be anchored at A, B, or C, giving rise to three different domains. Dark circles (trimers) mark Pt positions, smaller circles correspond to Si lattice atoms (refer to text for discussion).

Silicon samples were cut from a single-crystal wafer (As doped, 0.004–0.01 Ω cm) and cleaned *ex situ* by swaying in acetone, propanol, and methanol before introducing into the vacuum chamber. *In situ* preparation included outgassing for 12 h at moderate temperatures followed by a flash up to ~1250 °C until achieving a well-ordered surface, as evident from a clear (7×7) STM image. Between 1.0 and 1.5 ML of platinum (99.99% purity) was evaporated by an electron beam evaporator with the sample kept at room temperature. Subsequent and repeated annealing of the samples to ~900 °C resulted in a clear $\sqrt{3}$ low-energy electron diffraction (LEED) image. The preparation is robust with respect to excess Pt. During the annealing step, an extra amount of adsorbate seemingly desorbs or diffuses below the surface. According to Wawro *et al.*, Pt diffuses exceedingly into the Si substrate at its eutectic point (850 °C) with the $\sqrt{3}$ surface reconstructions remaining.[18] All STM measurements were performed at room temperature using the constant current mode.

III. STM OVERVIEW AND DOMAIN SIZE

The general nature of the $\sqrt{3}$-Pt/Si(111) is seen in the filled states STM image in Fig. 1. Apparently, the $\sqrt{3}$ domains exhibit a hexagonal array of one high intensity spot per unit cell. The surface periodicity, extracted from the present data, is derived as 6.7±0.1 Å with a typical corrugation of ~0.15 Å (see height profiles in Fig. 3). The value of 6.7 Å equals the lattice constant of a $\sqrt{3}$ reconstructed Si(111) surface. The individual domains are intersected by domain boundaries, recognizable by their darker contrast. The inset of Fig. 1 shows a model (with threefold rotational symmetry) of the upper three surface layers (Pt layer and two Si substrate layers). This illustrates, how three different domains may occur depending on whether the origin of the $\sqrt{3}$ unit cell is positioned at A, B, or C.

We find that the structure is very stable over a broad temperature range, as it persists on the surface up to 1000 °C. Repeated annealing cycles at various temperatures did not considerably change the surface topography or the domain size. According to prior studies, a change in the domain size due to further annealing was not observed.[17,18]

The domain boundaries are captured in more detail in the STM image of Fig. 2. The most striking features in this empty state image are the domain walls which show up as a network of bright lines whereas $\sqrt{3}$ domains appear darker. As a consequence, $\sqrt{3}$-Pt/Si(111) exhibits a lack of long-range order. The high density of domain walls results in rather small average domain sizes compared to other $\sqrt{3}$ systems. The distribution of domain sizes, shown in the inset of Fig. 2, is based on several single STM images. This statistical evaluation yields an average domain size of 10.2 nm^2, corresponding to ~35 Å×35 Å.

The atomic structure of domains and intersecting domain walls is observed in Fig. 3, showing both (a) filled and (b) empty states. This closer look unveils a phase shift between neighboring $\sqrt{3}$ domains, which are separated by phase-slip domain walls. The occurrence of phase-slip domains in $\sqrt{3}$-Pt/Si(111) has already been speculated about in LEED experiments due to an enlargement of fractional order spots.[14] The domain walls stretch like paths in three directions, which are rotated by 120° to another and pinned to the substrate geometry. In empty state images, the walls surmount the domain level by about 1 Å whereas in filled state images the contrast is reversed and the domains appear to be

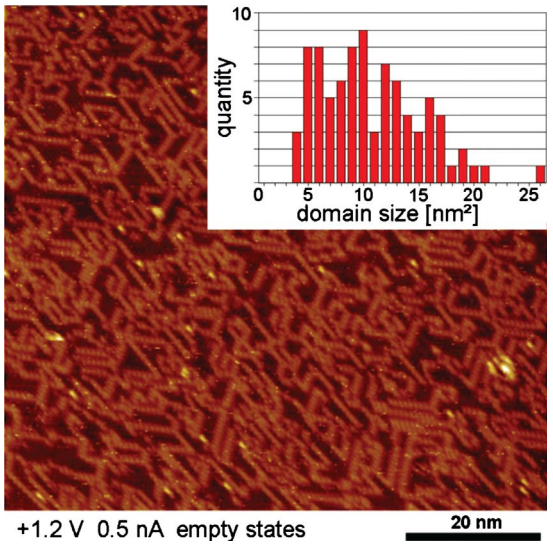

FIG. 2. (Color online) Domain walls of $\sqrt{3}$-Pt/Si(111) as seen in STM of empty states at +1.2 V bias (80×75 nm^2). Large parts of the surface are $\sqrt{3}$ reconstructed and intersected by domain walls, which appear as network of bright lines. The inset displays the distribution of the domain size (based on several STM measurements).

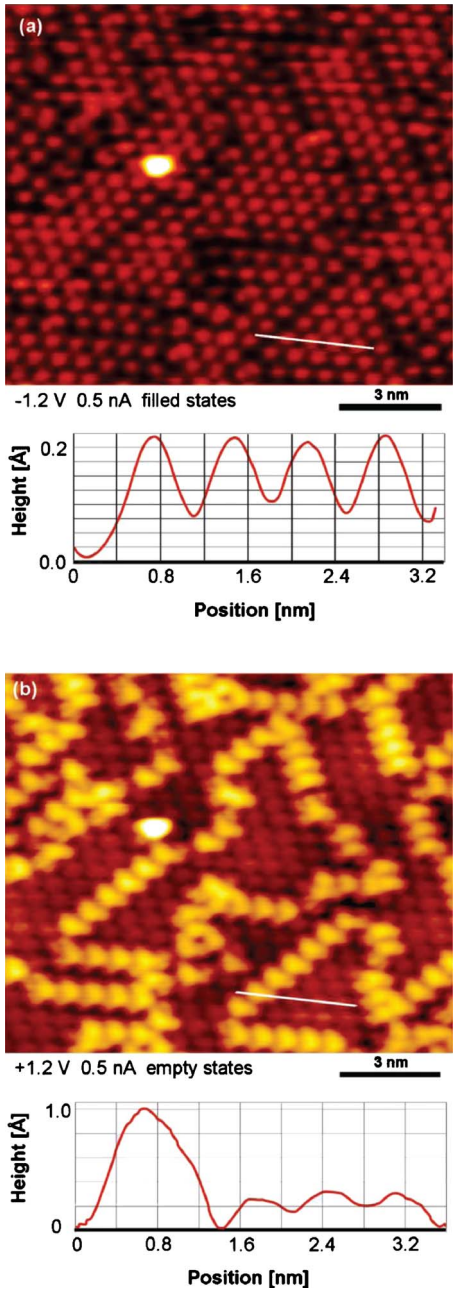

FIG. 3. (Color online) (a) Detailed domain and domain-wall analysis by STM at −1.2 V and (b) +1.2 V (13.5×11.5 nm^2). The commensurate $\sqrt{3}$ domains show up darker than the domain-wall network in the empty state image (b). Both images are taken at identical sample areas. Height profiles correspond to the white lines in the respective images. In-domain protrusions exhibit roughly the same height whereas the domain boundary, which is five times higher in empty states, is inverted in the filled states data.

elevated by ~0.15 Å above the walls. This is in accordance to the observations of Wawro *et al.*[17,18] This finding demonstrates that the contrast originates from the local density of states and does not represent a true topological structure. In contrast to the walls, the undulation inside of $\sqrt{3}$ domains does not strongly depend on bias (see line profiles in Fig. 3).

The above presented inspection of the $\sqrt{3}$-Pt/Si(111) surface reconstruction shows a clear resemblance to $\sqrt{3}$-Au/Si(111), which also exhibits a hexagonal pattern of $\sqrt{3}$ domains separated by a network of domain walls.[19–21] In contrast, $\sqrt{3}$-Ag/Si(111) shows notable differences, i.e., domain sizes, which are larger by a factor of ~50–100. Moreover, intensity maxima in empty states STM data at room temperature are arranged in a honeycomb pattern instead of a hexagonal pattern.[22]

With respect to the driving forces for domain formation, this high degree of disorder on a 10 nm scale in Pt/Si(111) is most probably due to a lattice mismatch between substrate and adsorbate. The bulk interatomic distance of Pt, $d_{\mathrm{Pt}}=2.78$ Å, deviates significantly from the corresponding value of Si, $d_{\mathrm{Si}}=2.35$ Å. This means a lattice mismatch of 18%, and it is highly plausible that domain-wall formation primarily will be due to strain. With respect to gold ($d_{\mathrm{Au}}=2.88$ Å) which is known to form domains of comparable size in $\sqrt{3}$-Au/Si(111), the deviation of substrate and adsorbate lattice constants is even larger. Here, domain sizes are highly dependent on the initial adsorbate coverage.[20] In contrast, $\sqrt{3}$-Ag/Si(111) exhibits huge domains, yet the bulk Ag lattice constant $d_{\mathrm{Ag}}=2.89$ Å is still close to d_{Au}. Therefore, one may exclude a correlation between bond lengths and strain-induced domain sizes.

Besides structural arguments, one may also consider the valence electronic properties. The orbital character of Au and Ag is again much more comparable to each other than to Pt. Both Au and Ag exhibit a full d shell and one single s electron whereas the electronic configuration of Pt is [Xe] $4f^{14}$ $5d^9$ $6s^1$. Therefore, Pt has an unpaired d electron and an essentially empty $6s$ shell, albeit that it may also be partially occupied as $d^{10-\delta}s^{\delta}$. Thus, since Pt has domains likewise, there is no straight forward correlation between orbital character and domain size.

A further attempt to explain the similarities and differences in the above stated triangular surface systems is considering their cohesion energies, as these display a measure for the energetic stability of an adsorbate. For one, Au exhibits a cohesion energy of about 5.8 eV whereas Ag is less stable (2.9 eV).[23] Second, Ag-Si bonds are energetically more preferential than Ag-Ag bonds.[24] These two facts seemingly correlate with large extended domains observed in experiment, rather than Ag clustering in form of domain boundaries. Pt however, exhibits a cohesion energy of 3.8 eV which is higher than the corresponding value of Ag but still far from the larger value of Au. Obviously, this energy is sufficient for the development of a dense network of domain walls.

Besides the discussion so far, the similarities between Au and Pt may also be related to their $5d$ orbitals. It has been suggested that due to relativistic effects, the d orbitals play an important role in surface bonding characteristics.[25] Observations in growth of one-dimensional atomic nanowires demonstrated that both Au and Pt react favorably with suitable semiconductor substrates whereas Ag does not.[26–28] This might be a hint toward similar chemical reactivity and wetting abilities of Au and Pt on the Si(111) substrate. The far-reaching $5d$ orbitals of both elements seemingly provide strong bondings to the substrate.

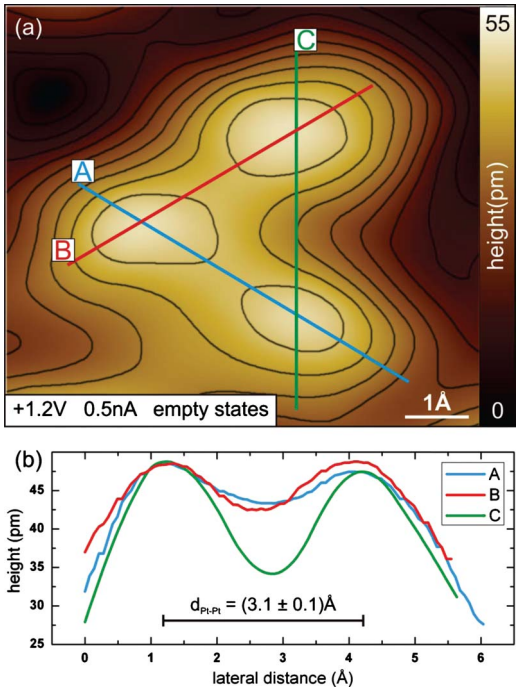

FIG. 4. (Color online) (a) Closeup STM image of a single *trimer* structure in the empty states at +1.2 V (0.74×0.66 nm^2) with black contour lines as a guide to the eyes. The triangular protrusion is reflected in the height profiles (b), taken along the straight lines in the STM image. Double Gaussian fits identify an average peak distance $d_{\text{Pt-Pt}}$=0.31 nm.

IV. STRUCTURAL BUILDING BLOCKS

A. Trimer units

After inspection of domains and the network of domain walls, a closeup of one single protrusion provides important insight for understanding of the atomic arrangement on the surface. Therefore, a detailed protrusion analysis is presented in Fig. 4. The empty states (bias+1.2 V) closeup of one triangular protrusion is scrutinized by contour plots along the lines, see Fig. 4(b). From the two peak positions (readout assisted by Gaussian fits), a Pt-Pt bond length $d_{\text{Pt-Pt}}=(3.1\pm0.1)$ Å is derived. Within the framework of the CHCT model, we ascribe this value to the Pt-Pt distance inside one *trimer*. The corresponding Au-Au bond length evaluated by Ding *et al.* is ~2.8 Å,[24] which almost equals the Au bulk next-neighbor distance (~2.9 Å). The difference between the corresponding Pt bulk next-neighbor distance (~2.8 Å) and the experimentally observed distance $d_{\text{Pt-Pt}}$ within *trimers* is only slightly larger. Hence, our experimental data and the Pt bulk spacing are in good agreement

This scenario is further supported by the observation of a bias-dependent change in the lateral protrusion shape in Fig. 5. In the (a) filled states, the protrusions appear merely oval, whereas in the (b) empty states, the apparent structure changes to a rather triangular shape. A comparison of protrusion shapes in both images with their corresponding electronic charge density is given in Fig. 5(c), according to calculations by Ding *et al.* for $\sqrt{3}$-Au/Si(111).[24] Importantly, these calculations rest upon the CHCT structure. As a guide to the eyes, the outer isocharge-density lines are overlaid on the STM data in Figs. 5(a) and 5(b). It follows that the main finding of our investigations is that the protrusions observed for different bias values originate from a platinum *trimer* instead of only a single atom, as proposed earlier by Wawro *et al.*[18] This finding necessarily implies a Pt coverage of 1 ML instead of 1/3 ML. In contrast to the CHCT model, where the Pt trimer apexes point toward adjacent trimers, our findings now unveil that the apexes point *in between* neighboring triangles. This consequently means that the Pt trimers are rotated by 30° from their locations in the pristine CHCT model, which is somewhat exceptional because it implies a *symmetry breaking* of the surface. This observation thus represents the remarkable finding of *chirality* at such semiconductor surface.

B. Domain-wall structure

Further key elements of the $\sqrt{3}$-Pt/Si(111) reconstruction can be unveiled by analyzing the domain-wall structure in detail. A suitable empty states STM image is presented in Fig. 6, showing domain walls, consisting of boomerang-shaped segments. The intersecting domain walls resemble much those observed in $\sqrt{3}$-Au/Si(111).[21] Furthermore, they exhibit a local $(2\times\sqrt{3})$ periodicity, as they are formed by two parallel rows of protrusions, each being part of neighboring $\sqrt{3}$ domains separated by twice the lattice constant of Si(111). A third parallel row is visible in between these columns. However, the protrusions of this third row are shifted by 2.2 Å in wall direction from an in line arrangement with the other two parallel rows, see inset of Fig. 6.

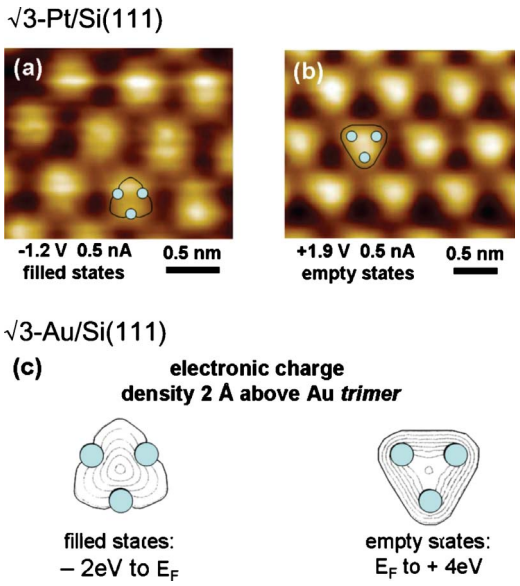

FIG. 5. (Color online) Analysis of protrusion shapes, comparing (a) filled states STM (2.0×1.8 nm^2) at −1.2 V and (b) empty states STM image (2.5×2.1 nm^2) at +1.9 V at the same site. (c) Comparison to the related system $\sqrt{3}$-Au/Si(111). Lateral protrusion shapes at different tunneling bias are shown for Au trimers with electronic charge densities calculated for the CHCT model by Ding *et al.* (Ref. 24).

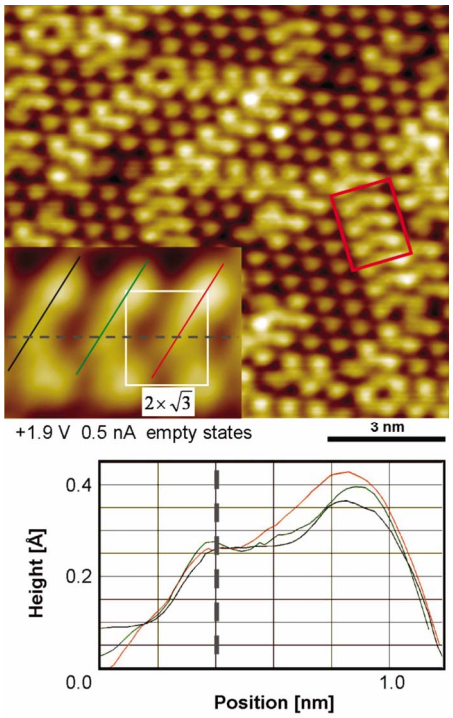

FIG. 6. (Color online) Domain-wall structure displayed in an empty states STM image (11.0×10.5 nm^2) at +1.9 V. The inset shows an enlargement of the domain-wall structure at the location indicated by the box. The $(2\times\sqrt{3})$ unit cell of the domain walls is displayed in white. The parallel lines correspond to the height profiles (*bottom*). In the center (dashed line) of each domain-wall segment, a third peak is observed.

According to the above results, one may derive a proposal for a structural model on the basis of the CHCT model, which includes the phase-slip domain walls. The methodical approach in this analysis is to use the domain boundaries to identify the orientation as well as the registry of the trimer units with respect to the substrate. In Fig. 7(a), an empty states STM image (U=+1.9 V) is overlaid by circles, representing single atomic positions. Each protrusion consists of three trimerized atoms, which are arranged in a $\sqrt{3}$ periodicity in the left domain . The right domain is shifted by Δ_2 =2.2 Å (1/3 of $\sqrt{3}$ lattice constant) with respect to the left one. The left and right domain-wall protrusion rows also consist of trimers, which are, however, in a distance of Δ_1 =7.7 Å, which is twice the Si(1×1) lattice constant instead of $\sqrt{3}$ times this distance. The shifted row in the middle of the domain wall is assumed to consist of only one Pt adatom per $(2\times\sqrt{3})$ unit cell due to its shape and smaller intensity in STM in comparison to the triangular shape of the trimers.

This domain-wall model is illustrated by Fig. 7(b), showing the topmost bilayer of Si(111) and the Pt adatoms. The trimer positions match very well the results from STM presented in Fig. 7(a) above. STM also reveals that the *single* atoms of the domain-wall middle row must be located on H_3 sites, as this position is the only one which conforms to the middle row shift of 2.2 Å (1/3 of $\sqrt{3}$ lattice constant). Comparing these empty state results with the filled states STM image in Fig. 1 demonstrates that there is no bias dependence regarding the domain-wall structure.

As a key signature, this model manifests the above reported chiral character of the surface, where enantiomeric domains must exist, with trimers rotated either 30° clockwise or counterclockwise (corresponding to left-handed and right-handed chirality). Note that this needs to be distinguished from domains as in Fig. 7 that result from a mere *registry shift*. This is in contrast to the results from $\sqrt{3}$-Au/Si(111). Moreover, in that surface system the domain-wall middle protrusions were attributed to Au *trimers* on H_3 sites (rather than single atoms). Thus, this modified CHCT configuration is the structural model to be favored in describing the atomic arrangement of $\sqrt{3}$-Pt/Si(111). One may speculate about the

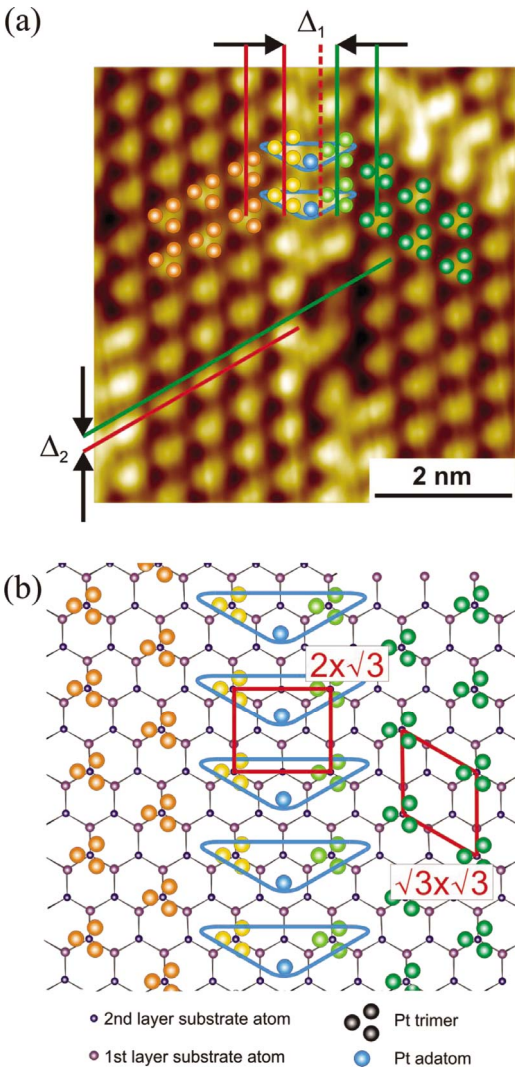

FIG. 7. (Color online) (a) Comparison of different phases in an empty states STM image (6.2×6.4 nm^2; +1.9 V; 0.5 nA) centered at a domain wall. Pt atom positions are overlaid by circles (*orange:* left domain; *green:* right domain; *yellow:* left domain wall; *bright green:* right domain wall; *blue* middle of domain wall). The triangles represent the boomeranglike shape of the domain wall protrusions. The straight lines illustrate phase shifts between the domains (Δ_1) and between trimer rows in both domains (Δ_2). (b) Domain-wall model, illustrating atom positions on a hexagonal substrate bilayer. Due to the phase shift, the domain walls exhibit a local $(2\times\sqrt{3})$ periodicity.

reasons of the trimer rotation. Possibly the allowed bond distance to the nearest Si atoms is altered in a favorable way, or more generally, lattice strain might locally be reduced. It follows from the (modified) CHCT model that the nominal Pt coverage is 1 ML for $\sqrt{3}$ reconstructed areas, as well as for domain walls. This also means that there exists no relation between the density of domain walls and adsorbate surface coverage.

Concerning the energetic stability, earlier studies on noble-metal-induced $\sqrt{3}$ reconstructions on Si(111) suggested the CHCT model to be energetically favorable. Ding *et al.* derived the *surface energy* of $\sqrt{3}$-Au/Si(111) with subject to the CHCT model to be lower than for the related honeycomb-chained-trimer (HCT) structure.[24] A further aspect is the presence of metal-metal bonds, which is typical of adatom trimers in CHCT systems such as Au/Si(111) and Pt/Si(111). These have a very high cohesive energy. In contrast, $\sqrt{3}$-Ag/Si(111) is characterized by strong Si bonds, which leads to a HCT surface structure. Concerning the electronic properties, metallic behavior was demonstrated by photoemission for $\sqrt{3}$-Au/Si(111).[29] Hence, one may speculate, whether $\sqrt{3}$-Pt/Si(111) is metallic, too. This issue may be addressed in future ARPES experiments.

V. CONCLUSIONS

In summarizing, the intriguing yet sparsely examined $\sqrt{3}$-Pt/Si(111) surface system was investigated using high-resolution STM at room temperature. Most parts of the surface are reconstructed in relatively small (10 nm^2) $\sqrt{3}$ domains, which are separated by phase-slip domain walls. The wall-to-domain height contrast is inverted when switching from empty to filled states, and vice versa. This indicates a topographic appearance in STM, which is highly influenced by the local charge density.[18] These structural attributes are reminiscent of $\sqrt{3}$-Au/Si(111).[21] Both Pt and Au exhibit a comparatively high cohesion energy, which is assumed to explain their similar behavior in structure and average domain size, which is in contrast to other $\sqrt{3}$ systems such as Ag/Si(111), that can grow on large areas without domains.[22]

The observed bias-dependent change in domain protrusion shape fits well to the $\sqrt{3}$-Au/Si(111) CHCT electronic charge-density calculations of Ding *et al.*[24] Furthermore, the Pt domain walls exhibit a local $(2\times\sqrt{3})$ periodicity with an additional protrusion in the center of the wall segment. Substantial evidence for a trimerized adsorption site of Pt is derived from a detailed protrusion substructure analysis. In fact, these observations are salient characteristics of a CHCT-like atomic arrangement.

However, contrary to the previously studied Au/Si(111) system, the trimers are rotated approximately 30° so that the surface symmetry is broken. As a consequence, the surface exhibits *chiral* character, which is rather unusual and has been rarely reported. The inequivalent triangle model is the only other candidate in this family of metal-semiconductor surface adsorbate systems that exhibits this feature, albeit weaker (only 6° rotation[30]). Also, there the assignment is based on density functional theory calculations while corresponding modeling for $\sqrt{3}$-Pt/Si(111) remains to be done. Other examples of chiral surfaces comprise, e.g., Si(110),[31] In clusters on Si(111),[32] high-index metal surfaces,[33] and oxygen-adsorbed Cu(110).[34] As a by-product of this study, mostly focused on structural and concomitant electronic properties, a chiral surface such as Pt/Si(111) may bear interesting properties for enantioselective adsorption of chiral organic molecules and for catalytic processes. It is a fascinating outlook to study these site-specific effects with STM.

ACKNOWLEDGMENTS

We acknowledge financial support from the Deutsche Forschungsgemeinschaft (FOR 1162 and Scha 1510/2-1). Furthermore, the authors are grateful to E. Tosatti for fruitful discussions about the physics of triangular lattices.

[1] J. M. Carpinelli, H. H. Weitering, E. W. Plummer, and R. Stumpf, Nature (London) **381**, 398 (1996).
[2] J. Falta, A. Hille, D. Novikov, G. Materlik, L. Seehofer, G. Falkenberg, and R. L. Johnson, Surf. Sci. **330**, L673 (1995).
[3] T. Hirahara, I. Matsuda, M. Ueno, and S. Hasegawa, Surf. Sci. **563**, 191 (2004).
[4] F. Gebhard, *The Mott Metal-Insulator Transition* (Springer-Verlag, Berlin, 1997).
[5] G. Grüner, *Density Waves in Solids* (Addison-Wesley, Reading, 1994).
[6] A. Mascaraque and E. G. Michel, J. Phys.: Condens. Matter **14**, 6005 (2002).
[7] R. I. G. Uhrberg, J. Phys.: Condens. Matter **13**, 11181 (2001).
[8] J. N. Crain, K. N. Altmann, C. Bromberger, and F. J. Himpsel, Phys. Rev. B **66**, 205302 (2002).
[9] G. Profeta and E. Tosatti, Phys. Rev. Lett. **98**, 086401 (2007).
[10] R. Cortés, A. Tejeda, J. Lobo, C. Didiot, B. Kierren, D. Malterre, E. G. Michel, and A. Mascaraque, Phys. Rev. Lett. **96**, 126103 (2006).
[11] S. Modesti, L. Petaccia, G. Ceballos, I. Vobornik, G. Panaccione, G. Rossi, L. Ottaviano, R. Larciprete, S. Lizzit, and A. Goldoni, Phys. Rev. Lett. **98**, 126401 (2007).
[12] G. Rossi, I. Abbati, L. Braicovich, I. Lindau, and W. E. Spicer, Phys. Rev. B **25**, 3627 (1982).
[13] G. Rossi, D. Chandesris, P. Roubin, and J. Lecante, Phys. Rev. B **34**, 7455 (1986).
[14] S. Okada, Y. Kishikawa, and T. Hanawa, Surf. Sci. **100**, L457 (1980).
[15] W. S. Yang, S. C. Wu, and F. Jona, Surf. Sci. **169**, 383 (1986).
[16] P. Morgen, M. Szymonski, J. Onsgaard, B. Jörgensen, and G. Rossi, Surf. Sci. **197**, 347 (1988).
[17] A. Wawro, S. Suto, and A. Kasuya, Phys. Rev. B **72**, 205302 (2005).
[18] A. Wawro, S. Suto, and A. Kasuya, Jpn. J. Appl. Phys. **45**, 2166 (2006).
[19] J. Nogami, A. A. Baski, and C. F. Quate, Phys. Rev. Lett. **65**,

1611 (1990).
[20] T. Nagao, S. Hasegawa, K. Tsuchie, S. Ino, C. Voges, G. Klos, H. Pfnür, and M. Henzler, Phys. Rev. B **57**, 10100 (1998).
[21] D. V. Gruznev, I. N. Filippov, D. A. Olyanich, D. N. Chubenko, I. A. Kuyanov, A. A. Saranin, A. V. Zotov, and V. G. Lifshits, Phys. Rev. B **73**, 115335 (2006).
[22] N. Sato, T. Nagao, and S. Hasegawa, Surf. Sci. **442**, 65 (1999).
[23] F. Kajzar and J. Mizia, J. Phys. F: Met. Phys. **7**, 1115 (1977).
[24] Y. G. Ding, C. T. Chan, and K. M. Ho, Surf. Sci. **275**, L691 (1992).
[25] R. H. M. Smit, C. Untiedt, A. I. Yanson, and J. M. van Ruitenbeek, Phys. Rev. Lett. **87**, 266102 (2001).
[26] J. Wang, M. Li, and E. I. Altman, Phys. Rev. B **70**, 233312 (2004).
[27] J. Schäfer, D. Schrupp, M. Preisinger, and R. Claessen, Phys. Rev. B **74**, 041404 (2006).
[28] J. Schäfer, C. Blumenstein, S. Meyer, M. Wisniewski, and R. Claessen, Phys. Rev. Lett. **101**, 236802 (2008).
[29] C. J. Karlsson, E. Landemark, L. S. O. Johansson, and R. I. G. Uhrberg, Phys. Rev. B **42**, 9546 (1990).
[30] H. Aizawa, M. Tsukada, N. Sato, and S. Hasegawa, Surf. Sci. **429**, L509 (1999).
[31] Y. Yamada, A. Girard, H. Asaoka, H. Yamamoto, and S. I. Shamoto, Phys. Rev. B **77**, 153305 (2008).
[32] J. H. Byun, J. S. Shin, P. G. Kang, H. Jeong, and H. W. Yeom, Phys. Rev. B **79**, 235319 (2009).
[33] A. Kara and T. S. Rahman, J. Phys.: Condens. Matter **18**, 8883 (2006).
[34] L. Guillemot and K. Bobrov, Phys. Rev. B **79**, 201406(R) (2009).